J Therm Anal Calorim (2009) 98:843–848
DOI 10.1007/s10973-009-0112-6

Thermodynamic properties of rubidium niobium tungsten oxide

Aleksandr Knyazev · Mirosław Mączka · Nataliya Kuznetsova · Jerzy Hanuza · Aleksey Markin

Received: 12 December 2008 / Accepted: 17 February 2009 / Published online: 10 June 2009

Abstract In the present work temperature dependence of heat capacity of rubidium niobium tungsten oxide has been measured first in the range from 7 to 395 K and then between 390 and 650 K, respectively, by precision adiabatic vacuum and dynamic calorimetry. The experimental data were used to calculate standard thermodynamic functions, namely the heat capacity $C_p^o(T)$, enthalpy $H^o(T) - H^o(0)$, entropy $S^o(T) - S^o(0)$, and Gibbs function $G^o(T) - H^o(0)$, for the range from $T \rightarrow 0$ to 650 K. The high-temperature X-ray diffraction and the differential scanning calorimetry were used for the determination of temperature and decomposition products of $RbNbWO_6$.

Keywords Adiabatic vacuum calorimetry · Differential scanning calorimetry · Heat capacity · Rubidium niobium tungsten oxide · Thermodynamic functions

Introduction

Materials with the crystal structure of pyrochlore, general formulation $A_2B_2O_6Y$, have been found to contain a wide variety of metal cations on both the A- and B-sites, e.g., lanthanide or alkali metal or alkaline earth cations on the A-site, and smaller cations that can adopt octahedral coordination (Ti^{4+}, Nb^{5+}, W^{6+}) on the B-site. Such materials have widespread applications including their use as ionic conductors [1], ferromagnetic [2], catalysts [3], and also for the immobilization of plutonium from dismantled nuclear weapons [4]. Thus perfect investigation of compounds with pyrochlore structure is especially significant.

Yet to understand the relations among structure, and energetics in a fundamental sense, and to address issues of reactivity at high temperature and materials compatibility in applications, thermodynamic data are essential. Despite the broad interest in tungsten pyrochlore, the only thermodynamic data have been reported previously in our article [5]. In the present work we report the results of the detailed thermodynamic investigation of $RbNbWO_6$.

The structure of $RbNbWO_6$ has been studied previously. The structure is built up of $(Nb/W)O_6$ octahedra, that share corners to form a three-dimensional framework possessing tunnels running down the *c*-axis in which the Rb cations are located. The Nb/W cations are located in the 16c Wyckoff sites (0, 0, 0) and the oxygen atoms are in 48f sites (0.312(1), 1/8, 1/8). The location of the rubidium cations is in the 8b sites (3/8, 3/8, 3/8) [6].

The goals of this work include calorimetric determination of the temperature dependence of the heat capacity $C_p^o = f(T)$ of rubidium niobium tungsten oxide from 7 to 650 K, detection of the possible phase transitions, and calculation of the standard thermodynamic functions $C_p^o(T)$, $H^o(T) - H^o(0)$, $S^o(T) - S^o(0)$, and $G^o(T) - H^o(0)$ in the range from $T \rightarrow 0$ to 650 K.

Electronic supplementary material The online version of this article (doi:10.1007/s10973-009-0112-6) contains supplementary material, which is available to authorized users.

A. Knyazev (✉) · N. Kuznetsova · A. Markin
Nizhny Novgorod State University, Gagarin Prospekt 23/2, 603950 Nizhny Novgorod, Russia
e-mail: knav@uic.nnov.ru

M. Mączka · J. Hanuza
Instutite of Low Temperature and Structure Research, Polish Academy of Sciences, P.O. Box 1410, 50-950 Wroclaw, Poland

Experimental

Sample

Rubidium niobium tungsten oxide was prepared by the solid-state reaction between tungsten oxide, niobium oxide, and rubidium nitrate [7]. The synthesis was performed in a porcelain crucible, into which the reaction mixture with the atomic ratio 1Rb: 1Nb: 1W was loaded. The mixture was calcined at 1173 K for 50 h, undergoing regrinding every 10 h.

X-ray diffraction pattern of a $RbNbWO_6$ sample was recorded on a Shimadzu X-ray diffractometer XRD-6000 (CuK_α radiation, geometry $\theta-2\theta$) in the 2θ range from 10° to 120° with scan increment of 0.02°. The X-ray data and estimated impurity content (0.5–1 wt%) in the substance led us to conclude that the rubidium niobium tungsten oxide sample studied was an individual crystalline compound.

Apparatus and measurement procedure

To measure the heat capacity C_p^o of the tested substance in the range from 7 to 395 K a BKT-3.0 automatic precision adiabatic vacuum calorimeter with discrete heating was used. The calorimeter design and the operation procedure were described earlier [8, 9]. The calorimeter was tested by measuring the heat capacity of high-purity copper and reference samples of synthetic corundum and K-2 benzoic acid. The analysis of the results showed that measurement error of the heat capacity of the substance at helium temperatures was within ±2%, then it decreased to ±0.5% as the temperature was rising to 40 K, and was equal to ±0.2% at $T > 40$ K. Temperatures of phase transitions can be determined with the error of ±0.02 K.

To measure the heat capacity of the sample between 390 and 650 K an automatic thermoanalytical complex (ADKTTM)—a dynamic calorimeter operating by the principle of triple thermal bridge—was used [10, 11]. The device design and the measurement procedure of the heat capacity, temperatures, and enthalpies of phase transitions were demonstrated in detail in the above-mentioned papers. The reliability of the calorimeter operation was checked by measuring the heat capacity of the standard sample of synthetic corundum as well as the thermodynamic characteristics of fusion of indium, tin, and lead. As a result, it was found that the calorimeter and the measurement technique allow one to obtain the heat capacity values of the substances in solid and liquid states with the maximum error of ±1.5% and the phase transition temperatures within *ca.* ±0.5 K. Since the heat capacity of the examined compound was also measured between 390 and 395 K in the adiabatic vacuum calorimeter with the error of ±0.2% and the conditions of measurements in the dynamic device were chosen so that in the above temperature interval the C_p^o values measured with the use of both calorimeters coincided, it was assumed that at $T > 395$ K the heat capacity was determined with the error of 0.5–1.5%. The data on the heat capacity of the object under study were obtained in the range from 390 to 650 K at the average rate of heating of the calorimeter and the substance of 0.0333 K/s.

Thermal behavior was carried out with DSC Labsys from Setaram in a corundum crucible ranging from 293 to 1573 K (heating rate 0.167 K/s).

Results and discussion

Heat capacity

The C_p^o measurements were carried out between 7 and 650 K. The masses of the sample loaded in the calorimetric ampoules of the BKT-3.0 and ADKTTM devices were 2.1235 and 2.0822 g, respectively. In the BKT-3.0 calorimeter, 282 experimental C_p^o values were obtained in two series of experiments. The heat capacity of the sample varied from 30% to 70% of the total heat capacity of calorimetric ampoule + substance over the range between 7 and 650 K. The experimental points of C_p^o in the temperature interval between $T =$ (7 and 650) K, except phase transitions field (350–370) K, were fitted by means of the least-squares method and polynomial equations of the C_p^o

Table 1 Coefficients in the fitting polynomials for $C_p^o = A + B\left(\frac{T}{30}\right) + C\left(\frac{T}{30}\right)^2 + D\left(\frac{T}{30}\right)^3 + E\left(\frac{T}{30}\right)^4 + F\left(\frac{T}{30}\right)^5 + G\left(\frac{T}{30}\right)^6$

T/K		7–30	25–150	130–350	370–650
Coefficients/ (J K^{-1} mol^{-1})	A	−0.66312	−30.737	−909.55	−6087.9
	B	9.5724	96.973	814.40	1940.0
	C	−85.904	−61.085	−271.16	−248.20
	D	469.25	27.436	47.847	16.833
	E	−755.36	−6.5809	−4.6519	−0.63762
	F	529.24	0.78570	0.23683	0.012844
	G	−139.61	−0.037031	−0.0049491	−0.00010828

vs. temperature have been obtained. The corresponding coefficients (A, B, C, etc.) are given in Table 1.

Their root mean square deviation from the averaging $C_p^o = f(T)$ curve was ±0.15% in the range T = (6–30) K, ±0.075% from T = (25 to 150) K, ±0.15% between T = (130 and 350) K and ±0.5% over the range from T = (370 to 650) K.

The experimental values of the molar heat capacity of $RbNbWO_6$ over the range from 7 to 650 K and the averaging $C_p^o = f(T)$ plot are presented in Fig. 1 and (Supplementary Table). The heat capacity C_p^o of this substance gradually increases with rising temperature and show two small anomalies at 356.5 and 361.6 K. The calculated enthalpy and entropy are 11.7 J mol^{-1} and 0.033 J mol^{-1} K^{-1} for the first phase transition and 10.8 J mol^{-1} and 0.030 J mol^{-1} K^{-1} for the second, respectively.

Perhaps, the presence of these transitions are connected with the existence of an intermediate phase between the paraelectric and ferroelectric phase [12].

Standard thermodynamic functions

To calculate the standard thermodynamic functions (Table 2) of the rubidium niobium tungsten oxide, its C_p^o values were extrapolated from the temperature of the measurement beginning at approximately 7 to 0 K by Debye's function of heat capacity:

$$C_p^o = nD(\theta_D/T), \quad (1)$$

where D is the symbol of Debye's function, $n = 5$ and $\theta_D = 101.8$ K are specially selected parameters. Eq. 1 with the above parameters describes the experimental C_p^o values of the compound between 7 and 12 K with the error of ±1.0%. In calculating the functions it was assumed that Eq. 1 reproduces the C_p^o values of $RbNbWO_6$ at $T < 7$ K with the same error. The calculations of $H^0(T) - H^0(0)$ and $S^o(T) - S^o(0)$ were made by the numerical integration of $C_p^o = f(T)$ and $C_p^o = f(\ln T)$ curves, respectively, and the Gibbs function $G^o(T) - H^o(0)$ was estimated from the enthalpies and entropies at the corresponding temperatures [13]. It was suggested that the error of the function values was ±1% at $T < 40$ K, ±0.5% between 40 and 80 K, ±0.2% in the range from 80 to 390 K and ±1.5% between 390 and 650 K.

The absolute entropies of rubidium niobium tungsten oxide (Table 2) and the corresponding simple substances W(cr), Nb (cr), Rb (cr) [14] and O_2 (g) [15] were used to calculate the standard entropy of formation of the compound under study at 298.15 K, $\Delta_f S°$ (298.15, $RbNbWO_6$, cr) = −538.5 ± 2.1 J K^{-1} mol^{-1}.

Differential scanning calorimetry

Rubidium niobium tungsten oxide decomposes at 1465 K. As can see from DSC curve (Fig. 2) we have summary endothermic effect. Thermal decomposition produces crystalline $Rb_{0.27}NbO_3$ and, probably, liquid $Rb_{0.73}WO_3$. $Rb_{0.27}NbO_3$ phase is identified by X-ray diffraction. Thus thermal decomposition may be represented by the following scheme:

$$RbNbWO_6(cr) \rightarrow Rb_{0.27}NbO_3(cr) + Rb_{0.73}WO_3(liq)$$

It can be seen from the suggested scheme that the studied compound has high thermal stability.

Conclusions

- The heat capacity for rubidium niobium tungsten oxide has been measured in the range from 7 to 650 K.
- From experimental data the standard thermodynamic functions of rubidium niobium tungsten oxide, namely,

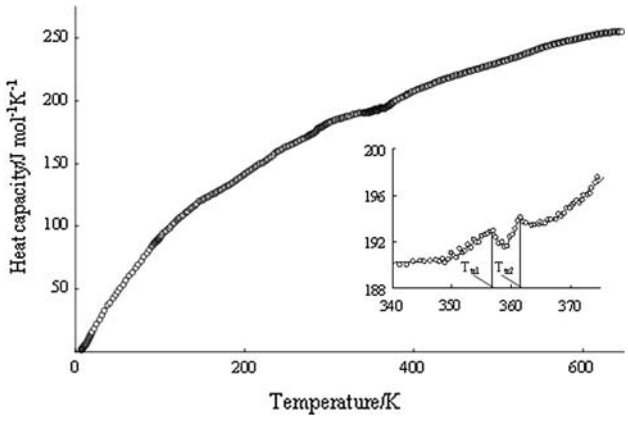

Fig. 1 Temperature dependence of heat capacity of $RbNbWO_6$

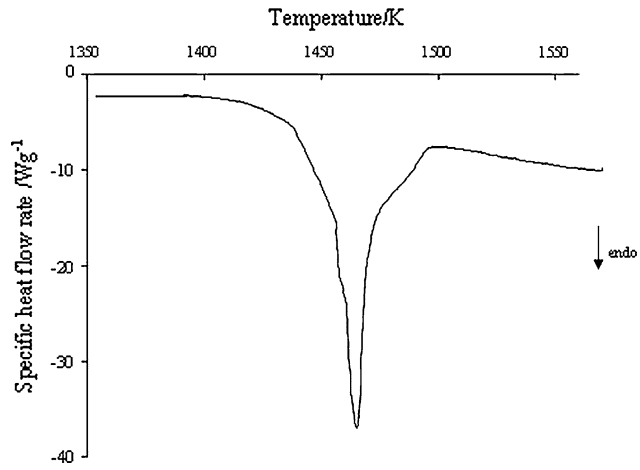

Fig. 2 Plot of the DSC-signal against temperature for $RbNbWO_6$

Table 2 Thermodynamic functions of crystalline $RbNbWO_6$; $M = 458.2206$ g mol^{-1}, p°= 0.1 MPa

T (K)	$C_p^o(T)$ (J K^{-1} mol^{-1})	$H^o(T) - H^o(0)$ (kJ mol^{-1})	$S^o(T) - S^o(0)$ (J K^{-1} mol^{-1})	$-[G^o(T) - H^o(0)]$ (kJ mol^{-1})
5	0.1931	0.00019	0.02254	0.000077
10	3.023	0.006573	0.8156	0.001583
15	8.453	0.03450	3.013	0.0107
20	14.80	0.09257	6.309	0.0336
25	20.88	0.1820	10.27	0.07488
30	26.52	0.3006	14.58	0.1369
35	31.95	0.4468	19.08	0.2210
40	37.27	0.6199	23.70	0.3280
45	42.38	0.8192	28.39	0.4581
50	46.97	1.043	33.09	0.6118
55	51.51	1.289	37.78	0.7890
60	55.85	1.557	42.45	0.9896
65	60.20	1.848	47.09	1.213
70	64.57	2.159	51.71	1.461
75	68.95	2.493	56.32	1.731
80	73.38	2.849	60.91	2.024
90	82.29	3.628	70.07	2.679
100	90.08	4.491	79.16	3.425
110	97.25	5.428	88.08	4.261
120	103.7	6.433	96.83	5.186
130	109.8	7.501	105.4	6.197
140	115.3	8.627	113.7	7.293
150	120.0	9.804	121.8	8.471
160	124.0	11.02	129.7	9.729
170	127.7	12.28	137.3	11.06
180	131.5	13.58	144.7	12.47
190	135.7	14.91	152.0	13.96
200	140.7	16.30	159.1	15.51
210	144.9	17.72	166.0	17.14
220	149.8	19.20	172.9	18.83
230	154.4	20.72	179.6	20.60
240	158.6	22.28	186.3	22.43
250	162.3	23.89	192.8	24.32
260	165.8	25.53	199.3	26.28
270	169.3	27.21	205.6	28.31
273.15	170.5	27.74	207.6	28.96
280	173.1	28.92	211.8	30.39
290	177.4	30.67	218.0	32.54
298.15	181.4	32.13	222.9	34.34
300	182.2	32.47	224.1	34.75
310	184.7	34.30	230.1	37.02
320	186.2	36.16	236.0	39.35
330	188.7	38.03	241.7	41.74
340	190.2	39.93	247.4	44.19
350	190.6	41.83	252.9	46.69
355	192.2	42.78	255.6	47.96
356	192.7	42.97	256.2	48.22
357	192.9	43.17	256.7	48.47

Table 2 continued

T (K)	$C_p^o(T)$ (J K^{-1} mol^{-1})	$H^o(T) - H^o(0)$ (kJ mol^{-1})	$S^o(T) - S^o(0)$ (J K^{-1} mol^{-1})	$-[G^o(T) - H^o(0)]$ (kJ mol^{-1})
358	191.9	43.36	257.2	48.73
359	191.5	43.55	257.8	48.99
360	192.6	43.74	258.3	49.25
361	193.6	43.94	258.8	49.51
362	193.7	44.13	259.4	49.76
363	193.5	44.32	259.9	50.02
364	193.5	44.52	260.4	50.28
365	193.7	44.71	261.0	50.55
370	195.0	45.68	263.6	51.86
380	199.6	47.65	268.9	54.52
390	203.5	49.67	274.1	57.23
400	206.9	51.72	279.3	60.00
410	209.8	53.81	284.5	62.82
420	212.4	55.92	289.5	65.69
430	214.8	58.05	294.6	68.61
440	217.1	60.21	299.5	71.58
450	219.2	62.40	304.4	74.60
460	221.4	64.60	309.3	77.67
470	223.4	66.82	314.1	80.79
480	225.6	69.07	318.8	83.95
490	227.7	71.33	323.5	87.16
500	229.8	73.62	328.1	90.42
510	232.0	75.93	332.7	93.72
520	234.1	78.26	337.2	97.07
530	236.3	80.61	341.7	100.5
540	238.5	82.99	346.1	103.9
550	240.6	85.38	350.5	107.4
560	242.6	87.80	354.8	110.9
570	244.6	90.23	359.2	114.5
580	246.5	92.69	363.4	118.1
590	248.3	95.16	367.7	121.8
600	249.9	97.66	371.8	125.5
610	251.3	100.2	376.0	129.2
620	252.6	102.7	380.1	133.0
630	253.5	105.2	384.1	136.8
640	254.3	107.8	388.1	140.7
650	254.7	110.3	392.1	144.6

the heat capacity $C_p^o(T)$, enthalpy $H^o(T) - H^o(0)$, entropy $S^o(T)$, and Gibbs function $G^o(T) - H^o(0)$ have been calculated for the range from $T \rightarrow 0$ to 650 K.

- The temperature and decomposition products of $RbNbWO_6$ were determinated.

Acknowledgments The work was performed with the financial support of NNSU's innovation educational program within the National project "Education".

References

1. Yamamura H, Nishino H, Kakinuma K, Nomura K. Electrical conductivity anomaly around fluorite–pyrochlore phase boundary. Solid State Ionics. 2003;158:359–65.
2. Chamberlain SL, Hess ST, Corruccini LR. Dipolar magnetic order in the pyrochlore structure. Phys Lett A. 2004;323:310–4.
3. Hashizume T, Yokota A, Saiki A, Terayama K. Fabrication of potassium tantalate films by hydrothermal electrochemical method at low temperature. J Therm Anal Calorim. 2008;92:431–4.

4. Yudintsev SV. Corrosion study of actinide waste forms with Garnet-type structure. Geol Ore Deposit. 2003;45:151–7.
5. Chernorukov N, Knyazev A, Kuznetsova N, Markin A, Smirnova N. Crystal structure and thermodynamic properties of cesium tantalum tungsten oxide. Thermochim Acta. 2008;470:47–51.
6. Bydanov NN, Chernaya TS, Muradyan LA, Sarin VA, Rider EE, Yankovskii VK, et al. Neutron-diffraction refinement of atomic structures of crystals of $RbNbWO_6$ and $TlNbWO_6$. Kristallografiya. 1987;32:623–30.
7. Babel D, Pausewang C, Viebahn W. Die Struktur einiger fluoride, oxide und oxidfluoride AMe_2X_6, der $RbNiCrF_6$ – Typ. Zeitschrift fuer Naturforschung, Teil B 1967;22:1219–20.
8. Varushchenko RM, Druzhinina AI, Sorkin EL. Low-temperature heat capacity of 1-bromoperfluorooctane. J Chem Thermodyn. 1997;29:623–7.
9. Malyshev VM, Milner GA, Sorkin EL, Shibakin VF. Automatic low-temperature calorimeter. Pribory i Tekhnika Eksperimenta. 1985;6:195–7.
10. Yagfarov MSh. New method of measuring the heat capacity and heat effects. Zh Fiz Khimii. 1969;43:1620–5.
11. Kabo AG, Diky VV. Details of calibration of a scanning calorimeter of the triple heat bridge type. Thermochim Acta. 2000;347:79–84.
12. Maczka M, Ko J-H, Wlosewicz D, Tomaszewski PE, Kojima S, Hanuza J, et al. Heat capacity and dielectric studies of ferroelectric superionic conductor $RbNbWO_6$. Solid State Ionics. 2004;167:309–15.
13. Lebedev BV. Application of precise calorimetry in study of polymers and polymerization processes. Thermochim Acta. 1997;297:143–9.
14. Chase MW Jr. NIST-JANAF themochemical tables, 4th ed. J Phys Chem Ref Data Monogr. 1998;9:1951 (database http://webbook.nist.gov/chemistry/).
15. Cox JD, Wagman DD, Medvedev VA. Codata key values for thermodynamics. New York; 1984 (database http://webbook.nist.gov/chemistry/).